

# Nanochitosan-Coated *Zingiber cassumunar* (Plai) for Anti-Inflammatory Applications: Characterization and Therapeutic Evaluation

Natthakamol Wakhuwathapong<sup>1,2</sup>, Pitchayapa Janyacharoen<sup>1,2</sup>, Nita Jungpichanwanit<sup>1,2</sup>, Sirichai Phinsiri<sup>2</sup>, Alisa Boonsuya<sup>2</sup>, Patpicha Arunsan<sup>2,5</sup>, Weerapat Foytong<sup>1</sup>, Nathkapach Kaewpitoon Rattanapitoon<sup>2,3</sup>, and Schawanya Kaewpitoon Rattanapitoon<sup>2,4</sup>, Chutharat Thanchonnang<sup>2,3,6\*</sup>

<sup>1</sup>Surawiwat School, Suranaree University of Technology, Nakhon Ratchasima, Thailand

<sup>2</sup>Parasitic Disease Research Center, Suranaree University of Technology, Nakhon Ratchasima, Thailand

<sup>3</sup>FMC Medical Center, Nakhon Ratchasima, Thailand

<sup>4</sup>School of Family Medicine and Community Medicine, Institute of Medicine, Suranaree University of Technology, Nakhon Ratchasima, Thailand

<sup>5</sup>Faculty of Medicine, Vongchavalitkul University, Nakhon Ratchasima, Thailand

<sup>6</sup>Translational Medicine program, Institute of Medicine, Suranaree University of Technology, Nakhon Ratchasima, Thailand

## Abstract

*Zingiber cassumunar* Roxb. (Plai), a traditional Thai medicinal plant, is widely recognized for its anti-inflammatory, analgesic, and antimicrobial properties. However, its clinical use has been limited due to poor solubility, stability, and skin permeability. This study aimed to develop and evaluate a nanochitosan-coated formulation incorporating *Zingiber cassumunar* (Plai) extract for anti-inflammatory applications. The study focuses on characterizing the physicochemical properties of the formulation using gas chromatography–mass spectrometry (GC-MS), Fourier transform infrared spectroscopy (FTIR), and scanning electron microscopy (SEM) techniques, as well as assessing its anti-inflammatory efficacy through the albumin denaturation assay.

The nanoparticles were characterized by GC-MS, FTIR, and SEM. GC-MS, and showed enrichment of lipophilic, volatile compounds like lidocaine, benzyl benzoate, and squalene. FTIR confirmed successful Plai incorporation into the chitosan matrix with strong molecular interactions. SEM revealed porous, sponge-like structures, supporting high drug-loading efficiency and potential for controlled release. Anti-inflammatory activity was assessed via BSA protein denaturation assay, revealing that all formulations, including crude extract, chitosan, and nanochitosan-Plai, exhibited high inhibition across tested concentrations. Notably, the nanochitosan-Plai formulation showed significantly superior activity at the highest concentration. These findings suggest that nanochitosan encapsulation significantly enhances the therapeutic efficacy of Plai, supporting its potential development as an advanced topical delivery system for the targeted management of localized inflammatory conditions. (International Journal of Biomedicine. 2025;15(3):564-571.)

**Keywords:** anti-inflammatory effect • nanochitosan • Plai • physical characterization

**For citation:**Wakhuwathapong N, Janyacharoen P, Jungpichanwanit N, Phinsiri S, Boonsuya A, Arunsan P, Foytong W, Rattanapitoon NK, Rattanapitoon SK, Thanchonnang C. Nanochitosan-Coated *Zingiber cassumunar* (Plai) for Anti-Inflammatory Applications: Characterization and Therapeutic Evaluation . International Journal of Biomedicine. 2025;15(3):564-571. doi:10.21103/Article15(3)\_OA18

## Abbreviations

**BSA**, bovine serum albumin; **DW**, distilled water; **FTIR**, Fourier transform infrared spectroscopy; **GC-MS**, gas chromatography–mass spectrometry; **SEM**, scanning electron microscopy.

## Introduction

*Zingiber cassumunar* Roxb., commonly referred to as Plai in Thailand, has been extensively used in Thai traditional medicine for the treatment of a variety of ailments, including muscle pain, sprains, inflammation, wounds, skin disorders, asthma, rheumatic conditions, and pain.<sup>1,2</sup> The essential Plai and rhizome extract of *Z. cassumunar* are known to exhibit local anesthetic and analgesic properties,<sup>3,4</sup> as well as potent anti-inflammatory effects.<sup>5</sup> Furthermore, antimicrobial studies have demonstrated that it possesses inhibitory activity against several bacterial and fungal strains,<sup>3</sup> reinforcing its value as a multifunctional herbal remedy. Moreover, *Z. cassumunar* has demonstrated a variety of biological activities,<sup>4</sup> including anti-inflammatory and analgesic effects, as well as ovicidal, insecticidal, cytotoxic, and antibacterial properties.<sup>6,7</sup> It has also exhibited potential in enzyme inhibition. Recent clinical studies further support the efficacy and safety of *Z. cassumunar* rhizome, particularly in reducing pain.<sup>8,9</sup>

The pharmacological efficacy of *Z. cassumunar* is largely attributed to its bioactive constituents, particularly terpinene-4-ol,  $\alpha$ -terpinene, and phenylbutenoids such as (E)-1-(3,4-dimethoxyphenyl)but-1-ene. These compounds have been shown to exert strong anti-inflammatory and analgesic effects in preclinical models, including carrageenan-induced paw edema and acetic acid-induced vascular permeability assays.<sup>10</sup> At the molecular level, extracts of *Z. cassumunar* have been reported to modulate key inflammatory signaling pathways. These phenylbutenoid compounds act as key bioactive indicators for quantifying herbal extracts,<sup>11</sup> emphasizing their therapeutic value in managing inflammation and supporting muscle recovery. The processes of extraction and standardization are essential in developing effective herbal preparations. Choosing an optimal extraction technique and an appropriate solvent is crucial for obtaining the highest yield of active ingredients, while standardization guarantees the reliability and consistency of therapeutic outcomes.

Despite these promising bioactivities, the clinical application of *Z. cassumunar* remains limited due to poor solubility, stability, and low skin permeability.<sup>2</sup> To overcome these limitations, nanocarrier systems have been explored to improve the delivery and bioavailability of phytochemicals.<sup>12,13</sup>

Chitosan, a natural biopolymer derived from chitin,<sup>14</sup> has emerged as a promising material for both systemic and localized drug and vaccine delivery. Its widespread use in pharmaceutical and biomedical fields is attributed to its excellent biocompatibility, biodegradability, and intrinsic bioactivity. Structurally similar to glycosaminoglycans, chitosan offers low toxicity and structural stability, making it less harmful to biological systems. Furthermore, it is easily broken down by enzymatic degradation, which enhances its safety profile. These properties make chitosan highly suitable for various therapeutic applications.<sup>15,16</sup> Chitosan-based nanoparticles, in particular, offer advantages such as biocompatibility, biodegradability, and mucoadhesive properties, making them suitable for topical drug delivery systems.<sup>17</sup> Prior studies have shown that encapsulating

herbal extracts,<sup>18</sup> including essential oils of *Z. cassumunar*, in chitosan nanoparticles enhances their physicochemical stability and facilitates.

In this study, a nanochitosan-based spray formulation incorporating *Z. cassumunar* extract was developed using the ionic gelation method. The formulation was characterized using Fourier-transform infrared spectroscopy (FTIR), gas chromatography–mass spectrometry (GC-MS), and scanning electron microscopy (SEM) to confirm its chemical integrity and particle morphology. The anti-inflammatory efficacy of the formulation was evaluated through albumin denaturation assays and compared with a standard reference drug, diclofenac. By integrating traditional herbal medicine with nanotechnology, this study proposes an innovative and effective topical therapy that enhances the therapeutic potential of *Z. cassumunar*. The findings support the development of safe, sustainable, and locally sourced alternatives for managing inflammation-related conditions.

## Materials and Methods

### Preparation of Chitosan Nanoparticles

Chitosan nanoparticles were prepared using the ionotropic gelation method.<sup>19–21</sup> Briefly, 0.25 g of sodium tripolyphosphate (TPP) (CAS Numbers: 7758-29-4) was dissolved in 250 mL of deionized water (DI) to serve as the cross-linking agent. Simultaneously, 0.1 g of chitosan (Lot Numbers: M13001) was dissolved in 5 mL of 1% acetic acid (CAS Numbers: 64-19-7), and subsequently diluted with 500 mL of DI water. The chitosan solution (475 mL) was then mixed with 25 mL of *Zingiber cassumunar* (Plai) crude extract (Batch: TS43Z1C21B) under continuous stirring at 500 rpm and 25°C for 1 hour using a magnetic stirrer. Following this, 250 mL of the TPP solution was added dropwise to the chitosan–Plai mixture, and the suspension was stirred for an additional 24 hours to facilitate nanoparticle formation. The mixture was left undisturbed to precipitate for 1 week, after which it was subjected to centrifugation at 10,000 rpm for five cycles, with purification conducted between each cycle to remove unbound components. The resulting product was stored at –80°C for 3 days, then freeze-dried to obtain the nanochitosan–Plai formulation in powder form.

### Characterization Analysis

#### Gas Chromatography–Mass Spectrometry (GC-MS) Analysis

The chemical composition of *Zingiber cassumunar* (Plai) crude extract was analyzed using GC-MS to identify its bioactive constituents. The extract was prepared at an appropriate concentration and subjected to analysis using an Agilent 7890A gas chromatograph coupled with an Agilent 7000B triple quadrupole mass spectrometer, operated via GC-QQQ software. Compound identification was performed using the NIST MS Search 2.0 library. For gas chromatography, the sample was injected using a liquid autosampler in split mode at a ratio of 5:1, with an injection volume of 2  $\mu$ L. The HP-5 capillary column (20 m  $\times$  0.18 mm, 0.18  $\mu$ m film thickness) was used for compound separation. The injection port and transfer line temperatures were set at 250°C, and helium

served as the carrier gas at a flow rate of 1.0 mL/min. In the mass spectrometer, ionization was achieved using electron ionization (EI) at 70eV. The ion source temperature was maintained at 230°C, and data were acquired in full scan mode over a mass range of 35–550.

### Fourier Transform Infrared Spectroscopy (FTIR) Analysis

Fourier transform infrared spectroscopy (FTIR) is an analytical technique used to identify chemical bonds and molecular structures by measuring the absorption of infrared radiation at various wavelengths. In this study, nanochitosan-Plai samples were characterized using FTIR with a Vertex 70 instrument (Bruker, Switzerland; Serial No. 3099/HYP.1097). Spectra were recorded at a resolution of 4 cm<sup>-1</sup>, with 64 scans performed for both the sample and the background. Each analysis was repeated at least three times to ensure reproducibility. Data acquisition and processing were carried out using OPUS software.

### Characterization using Scanning Electron Microscopy (SEM) Analysis

The morphology of nanochitosan-Plai nanoparticles was examined using SEM to assess their surface structure, particle shape, and distribution. Freeze-dried samples were carefully mounted on aluminum stubs and sputter-coated with a thin layer of gold to enhance conductivity. Imaging was performed using a JEOL JSM-6010LV SEM system, equipped with Energy Dispersive X-ray Spectroscopy (EDS) for elemental analysis. SEM micrographs were captured at appropriate magnifications to reveal the porous, aggregated morphology and irregular surface features typical of nanochitosan-based formulations. These morphological insights were critical for evaluating the physical characteristics and structural stability of the nanoparticles.

### Anti-Inflammatory Activity

The anti-inflammatory activity of the test samples was evaluated using the Bovine Serum Albumin (BSA) (CAS Numbers: 9048-46-8) protein denaturation method.<sup>22</sup> A 5% BSA solution (CAS No. 9048-46-8) was prepared in distilled water. Test samples included Diclofenac sodium (positive control), chitosan (dissolved in 0.05% acetic acid), Plai crude extract, and nanochitosan-Plai formulation. Each sample was prepared at six concentrations: 25, 50, 100, 200, 500, and 1000 µg/mL. For each concentration, 1 mL of the test solution was mixed with 1 mL of the 5% BSA solution and incubated at 27°C for 15 minutes. A control solution consisting of BSA and distilled water (DW) was also prepared. After incubation, the mixtures were heated at 70°C for 10 minutes to induce protein denaturation. The samples were then cooled to room temperature, and the absorbance was measured at 660 nm using a VICTOR® Nivo™ Multimode Plate Reader (Serial No. HH35L2020289).

The percentage of protein denaturation inhibition, indicating anti-inflammatory activity, was calculated using the following formula:<sup>23</sup>

$$\% \text{Inhibition} = \frac{\text{Absorbance of control} - \text{Absorbance of sample}}{\text{Absorbance of control}} \times 100$$

### Statistical analysis

All data are presented as mean ± standard deviation (SD). Statistical comparisons between groups were conducted using one-way ANOVA. A probability value  $P \leq 0.05$  was considered statistically significant.

## Results

### Gas Chromatography–Mass Spectrometry (GC-MS) Analysis

Gas chromatography–mass spectrometry (GC–MS) analysis was conducted to compare the chemical constituents of Zingiber cassumunar (Plai) crude extract and the nanochitosan-Plai formulation. The chromatogram of the crude Plai extract in Table 1 was dominated by hydrophilic and solvent-derived compounds, with propylene glycol comprising 69.42% of the total peak area, followed by 1,3-butanediol (22.80%) and ethanol, 2-phenoxy- (5.77%). These compounds, often used as cosolvents in herbal extraction, were accompanied by a diverse range of minor bioactive compounds, including vanillin, Zingiberone, β-sesquiphellandrene, and several saturated and unsaturated fatty acids, such as oleic acid, octadecanoic acid, and n-hexadecanoic acid.

Notably, DMPBD (detected at RT 25.986, 0.18%) was also present, which may represent a bioactive aromatic derivative contributing to the therapeutic profile of Plai. In contrast, the nanochitosan-Plai formulation in Table 2 exhibited a distinctly different chemical profile, enriched in hydrophobic and volatile components. Major peaks included lidocaine benzyl benzoate (15.35%), phenol, 2,4-bis(1,1-dimethylethyl)- (9.86%), tetradecane (6.98%), dodecane (6.86%), and benzene, 1,3-bis(1,1-dimethylethyl)- (6.69%). Alkanes such as undecane, hexadecane, octadecane, and eicosane were also abundant, along with squalene (2.87%), a compound known for its emollient and antioxidant activity. Many of these hydrophobic compounds were not detected in the crude extract, suggesting that the nanoencapsulation process enhanced the retention or solubilization of lipophilic constituents. This chemical shift may be attributed to interactions with the chitosan matrix, improved compound stability, or differences in extraction and formulation conditions. The presence of new or more prominent bioactive compounds in the nanoparticle formulation supports the potential of nanochitosan-based delivery systems to enhance the therapeutic efficacy and skin permeability of Plai extract for topical or transdermal applications.

### Fourier Transform Infrared Spectroscopy (FTIR) Analysis

FTIR spectrum of the nanochitosan-Plai formulation revealed the presence of distinct absorption bands indicating various functional groups. A broad absorption band observed around 3400 cm<sup>-1</sup> corresponds to the stretching vibrations of O–H and N–H groups, confirming the presence of hydroxyl and amine functionalities from both chitosan and plant-derived compounds. Peaks near 2920 cm<sup>-1</sup> and 2850 cm<sup>-1</sup> are associated with aliphatic C–H stretching vibrations. A noticeable band around 1650 cm<sup>-1</sup> can be attributed to C=O stretching from amide I, while a peak near 1580 cm<sup>-1</sup> suggests N–H bending (amide II), both of which are characteristic of chitosan (Figure 1).

Table 1.

**Chemical constituents identified in the *Zingiber cassumunar* (Plai) crude extract using GC-MS.**

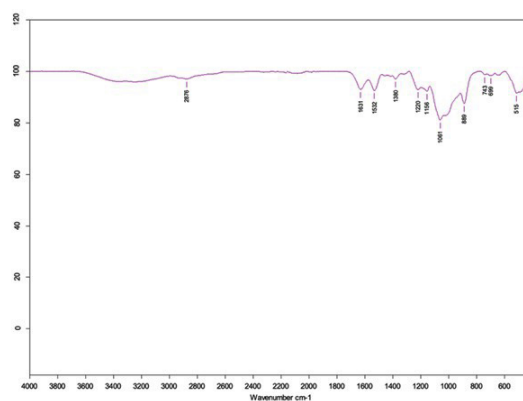
RT	Area	Area Sum %	Name
10.739	1271088634	69.42	Propylene Glycol
11.671	417481384	22.80	1,3-Butanediol
12.013	168629	0.01	Ethanol, 2,2'-oxybis-
12.532	485358	0.03	2-Propanol, 1,1'-oxybis-
12.749	972462	0.05	1,3-Pentanediol, 2,2,4-trimethyl-
12.824	294261	0.02	2,4-Pentanediol, 3-methyl-
15.208	105582383	5.77	Ethanol, 2-phenoxy-
17.261	61528	0.00	n-Decanoic acid
17.770	155176	0.01	Vanillin
18.632	57340	0.00	Octanoic acid, methyl ester
19.013	80874	0.00	Benzaldehyde, 3,4-dimethoxy-
19.225	375999	0.02	Tetraethylene glycol
19.672	120374	0.01	$\beta$ -Sesquiphellandrene
20.296	894806	0.05	Dodecanoic acid
20.679	687543	0.04	2-Allyl-1,4-dimethoxy-3-methyl-benzene
21.077	57051	0.00	Zingiberone
21.246	3520335	0.19	Triquinacene, 1,4-bis(methoxy)-
21.575	70805	0.00	Decanoic acid, methyl ester
22.440	122403	0.01	1,4,7,10,13,16,19-Heptaosa-2-cycloheptacosanone
23.017	120653	0.01	Cinnamic acid, 3,4-dimethoxy-, methyl ester
23.044	115816	0.01	Tetradecanoic acid
23.179	327377	0.02	Hexaethylene glycol
23.685	758751	0.04	Triquinacene, 1,4,7-tris(methoxy)-
24.286	415809	0.02	Dodecanoic acid, 3-hydroxypropyl ester
24.356	169599	0.01	Lauric anhydride
24.433	3111723	0.17	1,2-Dimethoxy-4-(3-methoxy-1-propenyl)benzene
24.614	127560	0.01	2(3H)-Furanone, 3-heptyldihydro-
25.653	673595	0.04	n-Hexadecanoic acid
25.743	336829	0.02	Dodecanoic acid, 1-methylpropyl ester
25.986	3363567	0.18	DMPBD
26.833	6440897	0.35	13-Hexyloxacyclotridecan-2-one
26.896	286183	0.02	Glycerol 1-myristate
28.001	649561	0.04	Oleic Acid
28.376	1546720	0.08	Octadecanoic acid
28.497	131795	0.01	Stearic acid, 2-hydroxy-1-methylpropyl ester
29.739	125525	0.01	Glycerol $\beta$ -palmitate
30.787	468867	0.03	Heptaethylene glycol
31.172	1456882	0.08	12-Hydroxystearic acid
32.677	105111	0.01	Glyceryl 1-monostearate
33.575	145933	0.01	Diisooctyl phthalate
34.790	653620	0.04	Octaethylene glycol
38.237	1863599	0.10	2-Undecenoic acid, trimethylsilyl ester
39.898	1538073	0.08	4,7-Dimethoxy-2-methyl-1H-indene
40.424	1513850	0.08	4,7-Dimethoxy-2-methyl-1H-indene
41.738	1232807	0.07	1-Methyl-1-(5-tridecyl)oxy-1-silacyclopentane
42.302	537068	0.03	Nonaethylene glycol
43.123	140544	0.01	Stigmasterol
44.160	338163	0.02	$\beta$ -Sitosterol
Total	1830973822	100	

Table 2.

**Chemical constituents identified in the nanochitosan-Plai using GC-MS.**

RT	Area	Area Sum %	Name
10.121	133871	3.48	Decane
10.631	59535	1.22	Octane, 3,3-dimethyl-
11.394	203810	4.17	Undecane, 5,7-dimethyl-
12.278	145782	2.98	Undecane
14.072	97856	2.00	1-Dodecene
14.230	335476	6.86	Dodecane
15.222	326928	6.69	Benzene, 1,3-bis(1,1-dimethylethyl)-
17.606	78302	1.60	1-Tetradecene
17.731	341523	6.98	Tetradecane
19.545	482228	9.86	Phenol, 2,4-bis(1,1-dimethylethyl)-
20.782	278281	5.69	Hexadecane
23.521	201634	4.12	Octadecane
26.041	119315	2.44	Eicosane
26.139	80801	1.65	Indazol-4-one, 3,6,6-trimethyl-1-phthalazin-1-yl-1,5,6,7-tetrahydro-
28.717	74171	1.52	Docosane
33.284	750788	15.35	Lidocaine benzyl benzoate
37.444	140551	2.87	Squalene
Total	3850852		

Additionally, peaks between 1150 and 1020  $\text{cm}^{-1}$  correspond to C–O–C and C–O stretching vibrations, indicating saccharide structures and ether linkages. The presence of these characteristic bands confirms the successful incorporation of *Zingiber cassumunar* extract into the chitosan matrix and suggests potential hydrogen bonding or molecular interactions between chitosan and bioactive compounds in the extract. The resulting FTIR spectrum is consistent with the formation of a stable nanoformulation containing phytochemically active components.



**Fig. 1.** FT-IR spectrum and chemical formula of nanochitosan-Plai.

### Scanning Electron Microscopy (SEM) Analysis

Scanning electron microscopy (SEM) analysis was performed to observe the surface morphology and structural



characteristics of the nanochitosan-Plai formulation. At low magnification (Fig. 2 (a), 100 $\times$ ), the surface displayed randomly distributed, irregular aggregates with a flaky and rough texture. The particles were widely scattered and varied in size, indicating that the formulation was composed of heterogeneous agglomerates formed during the drying or preparation process. At high magnification (Fig. 2 (b), 30,000 $\times$ ), the morphology of the nanoparticles was more distinctly revealed. The image showed porous, sponge-like structures with uneven surfaces, characteristic of chitosan-based nanomaterials. The nanostructured morphology and rough surface suggested increased surface area, which may enhance drug loading and facilitate controlled release. These morphological features confirm that the nanochitosan effectively encapsulated the *Zingiber cassumunar* extract, forming a stable nanosystem suitable for transdermal or topical delivery.

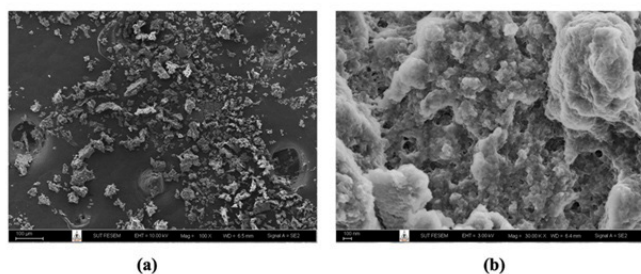


**Fig. 2.** Scanning Electron Microscopy (SEM) images of nanochitosan-Plai formulation at different magnifications:

(a) Low magnification (100 $\times$ ) showing dispersed and irregularly shaped aggregated particles scattered across the substrate surface.

(b) High magnification (30,000 $\times$ ) revealing porous, rough, and sponge-like nanostructures with interconnected networks, indicative of successful encapsulation and nanoscale morphology.

### Anti-Inflammatory Activity

The anti-inflammatory activity, as evaluated by the BSA protein denaturation assay, revealed that all four tested formulations, Diclofenac (positive control), *Zingiber cassumunar* (Plai) extract, chitosan, and the nanochitosan-Plai formulation, exhibited high levels of inhibition across all tested concentrations (25–1000  $\mu\text{g/mL}$ ), with values consistently exceeding 90%. This suggests that both the crude and nanoformulated versions of Plai, as well as chitosan alone, possess substantial anti-inflammatory potential, likely due to their bioactive phenolic and terpenoid constituents and, in the case of chitosan, its inherent bioadhesive and modulatory properties. Although the inhibition values were numerically close across groups, a statistically significant difference ( $P=0.003$ ) was observed at the highest concentration (1000  $\mu\text{g/mL}$ ), where the nanochitosan-Plai formulation demonstrated superior inhibition compared to the other groups. This enhanced effect at higher concentrations may be attributed to the improved stability, solubility, and sustained release properties of the nanoformulated system, which likely increase the bioavailability of the active compounds in Plai. At lower concentrations (25–500  $\mu\text{g/mL}$ ), there were no significant differences among the groups ( $P>0.05$ ), indicating

that the anti-inflammatory effect of Plai is already pronounced even without nanoencapsulation. However, the marginal improvements seen with the nanochitosan formulation suggest a trend toward greater efficacy, particularly at higher doses, as shown in Fig. 3. Overall, the results support that nanochitosan-Plai retains the potent anti-inflammatory activity of the crude extract and may offer advantages in terms of delivery and therapeutic performance, especially when applied in formulations requiring enhanced stability and skin penetration, such as transdermal sprays or topical films.

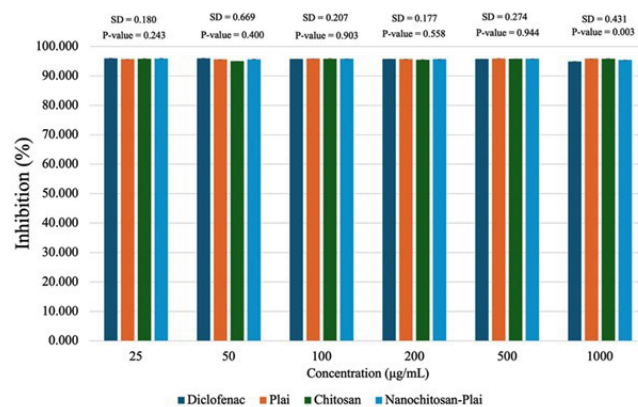


**Fig. 3.** Percentage inhibition of anti-inflammation activity for Diclofenac, Plai extract, Chitosan, and Nanochitosan-Plai formulations at different concentrations (25–1000  $\mu\text{g/mL}$ ). The results are expressed as mean inhibition percentages ( $n = 3$ ) with standard deviations shown above each group. Statistical analysis using ANOVA indicates no significant differences between groups at concentrations of 25–500  $\mu\text{g/mL}$  ( $P > 0.05$ ), while a significant difference was observed at 1000  $\mu\text{g/mL}$  ( $P = 0.003$ ), where the Nanochitosan-Plai formulation exhibited the highest anti-inflammatory activity.

The anti-inflammatory activity of the nanochitosan-Plai formulation was evaluated using the BSA protein denaturation assay, a well-established model for assessing the stabilization of protein structures under inflammatory conditions. All tested groups, including diclofenac (positive control), *Z. cassumunar* (Plai) extract, chitosan, and the nanochitosan-Plai formulation, exhibited high levels of protein denaturation inhibition ( $>90\%$ ) across all tested concentrations (25–1000  $\mu\text{g/mL}$ ). These results highlight the inherent anti-inflammatory potential of both the Plai extract and chitosan polymer. Interestingly, while the inhibition rates among groups were closely matched at lower concentrations (25–500  $\mu\text{g/mL}$ ), no statistically significant differences were found ( $P>0.05$ ), indicating that the crude extract of *Z. cassumunar* already possesses strong anti-inflammatory activity, consistent with previous reports attributing this to the presence of active compounds such as terpinene-4-ol, sabinene, and (E)-1-(3,4-dimethoxyphenyl)but-1-ene.<sup>10</sup> However, at the highest tested concentration (1000  $\mu\text{g/mL}$ ), the nanochitosan-Plai formulation significantly outperformed the other groups ( $P=0.003$ ), demonstrating a clear enhancement of bioactivity in a dose-dependent manner.

## Discussion

In this study, a nanochitosan-based formulation incorporating *Zingiber cassumunar* (Plai) extract was successfully developed using the ionic gelation technique. The formulation underwent comprehensive characterization via GC-MS, FTIR, SEM, confirming its chemical composition and nanoparticulate morphology. Anti-inflammatory potential was assessed through albumin denaturation assays, with diclofenac serving as the reference drug. The integration of traditional herbal medicine with nanotechnology presents a promising strategy for enhancing topical therapeutic efficacy. These results underscore the potential of this formulation as a safe, sustainable, and locally derived anti-inflammatory agent.

The GC-MS analysis of *Zingiber cassumunar* (Plai) crude extract and nanochitosan-Plai formulation revealed distinct differences in chemical profiles, suggesting that nanoencapsulation significantly influences compound retention and presentation. In the crude extract, the dominant components were hydrophilic and solvent-associated compounds such as propylene glycol (69.42%), 1,3-butanediol (22.80%), and ethanol, 2-phenoxy- (5.77%), consistent with earlier studies that reported alcohols and glycols as major constituents when hydroalcoholic or aqueous extractions were used.<sup>24,25</sup> Minor but therapeutically relevant compounds such as Zingiberone,  $\beta$ -sesquiphellandrene, vanillin, and unsaturated fatty acids (e.g., oleic and octadecanoic acids) were also identified, aligning with previous findings that Plai contains phenylbutenoids, sesquiterpenes, and aromatic ketones with anti-inflammatory activity.<sup>26</sup>

Notably, the nanochitosan-Plai formulation exhibited a shift toward lipophilic and volatile constituents, such as lidocaine benzyl benzoate (15.35%), phenol, 2,4-bis(1,1-dimethylethyl)- (9.86%), and a range of alkanes (e.g., tetradecane, hexadecane, and octadecane), which were not prominent in the crude extract. These findings suggest that the nanoencapsulation process may selectively retain or stabilize volatile and hydrophobic compounds, as reported by similar studies on nanoemulsions and chitosan-based delivery systems. The appearance of squalene (2.87%), a known antioxidant and skin-conditioning agent, further supports the enhanced bioactive profile achieved through nanoformulation. Moreover, the detection of DMPBD (0.18%) in the crude extract is in line with previous work reporting dimethoxyphenyl derivatives as contributors to Plai's anti-inflammatory effects.<sup>26</sup>

Overall, the chemical shift observed between crude and nanoformulated Plai suggests that chitosan-based nanoencapsulation not only protects the active phytochemicals but also potentially enhances the formulation's stability, bioavailability, and skin permeability. These results are consistent with prior research on nanocarrier systems improving the pharmacological potential of herbal compounds and highlight the nanochitosan-Plai formulation as a promising candidate for transdermal or topical therapeutic applications.

Fourier Transform Infrared Spectroscopy (FTIR) was used to confirm the successful incorporation of *Zingiber*

*cassumunar* extract into the chitosan-based nanoparticle system and to identify possible molecular interactions between the extract and the polymer matrix. The FTIR spectrum of chitosan exhibited characteristic peaks at 3430  $\text{cm}^{-1}$  (O-H and N-H stretching), 2920 and 2850  $\text{cm}^{-1}$  (C-H stretching), 1650  $\text{cm}^{-1}$  (C=O stretching of amide I), and 1580  $\text{cm}^{-1}$  (N-H bending of amide II), which are consistent with previous reports describing chitosan's functional groups.<sup>27</sup> Additionally, peaks between 1150 and 1020  $\text{cm}^{-1}$  corresponded to C-O-C and C-O stretching vibrations typical of saccharide structures. The spectrum of crude *Z. cassumunar* showed strong bands in the range of 3400–3300  $\text{cm}^{-1}$  attributed to O-H stretching and in the fingerprint region (1000–1500  $\text{cm}^{-1}$ ) related to phenolic, aromatic, and terpene structures, consistent with its known phenylbutenoid and sesquiterpene content.<sup>28</sup> These phytochemical groups are largely responsible for Plai's reported anti-inflammatory, analgesic, and antioxidant properties.<sup>4</sup>

In the nanochitosan-Plai composite formulation, the FTIR spectrum retained major absorption bands from both chitosan and Plai but with shifts in peak positions and changes in intensity particularly in the amide I (1650  $\text{cm}^{-1}$ ) and C-O stretching (1020–1100  $\text{cm}^{-1}$ ) regions suggesting strong hydrogen bonding or electrostatic interactions between the polymer and the phytoconstituents. Such interactions are commonly observed in chitosan-based nanocarriers and have been shown to enhance the chemical stability and bioavailability of encapsulated herbal compounds.<sup>13</sup> Overall, the FTIR results confirm the formation of a chemically stable nanoformulation, wherein the bioactive compounds from *Z. cassumunar* were effectively incorporated into the chitosan-PVA-glycerin matrix. These findings are in agreement with prior studies demonstrating that chitosan nanoparticles can successfully encapsulate essential and improve their delivery characteristics, including controlled release, enhanced skin permeability, and increased therapeutic potential.<sup>5</sup>

Morphological analysis using Scanning Electron Microscopy (SEM) revealed the nanochitosan-Plai particles to have rough, porous, sponge-like structures at high magnification (30,000 $\times$ ), a characteristic typical of chitosan-based nanocarriers. These structural features not only confirm successful encapsulation but also suggest improved drug-loading capacity and potential for controlled release. The irregular aggregates observed at low magnification (100 $\times$ ) suggest particle agglomeration during drying, which is common in spray or solvent evaporation methods. Similar SEM morphologies have been documented in other studies involving chitosan nanoparticles and support their utility in enhancing transdermal drug delivery.<sup>29</sup>

These findings align with prior studies indicating that nanoencapsulation can enhance the therapeutic efficacy of herbal actives by improving their permeability and retention in biological tissues, especially in transdermal or topical applications. Therefore, the nanochitosan-Plai formulation not only maintains but potentially augments the anti-inflammatory efficacy of crude Plai extract, making it a promising candidate for next-generation drug delivery systems targeting localized inflammation.

## Conclusions

In this study, a nanochitosan-based formulation incorporating *Zingiber cassumunar* (Plai) extract was successfully developed using the ionic gelation technique. Comprehensive characterization using gas chromatography–mass spectrometry (GC–MS), Fourier-transform infrared spectroscopy (FTIR), and scanning electron microscopy (SEM) confirmed the chemical composition and nanoparticulate morphology of the formulation. The anti-inflammatory potential was evaluated through the albumin denaturation assay, with diclofenac used as a reference drug. GC–MS analysis revealed that nanoencapsulation significantly altered the chemical profile, enriching the formulation with lipophilic and volatile constituents such as lidocaine, benzyl benzoate, squalene, and alkanes, which were either absent or present in low concentrations in the crude extract. These findings suggest that the nanocarrier system helps retain and stabilize bioactive compounds, thereby enhancing therapeutic potential. FTIR analysis confirmed successful incorporation of *Z. cassumunar* extract into the chitosan matrix, as indicated by the presence of characteristic functional group bands from both the polymer and the extract. Shifts in peak positions and intensity suggested hydrogen bonding or electrostatic interactions, which are commonly associated with improved chemical stability and bioavailability in nanocarrier systems. SEM images revealed porous, rough, sponge-like structures typical of chitosan nanoparticles, supporting efficient drug loading and controlled release capabilities. The observed morphological characteristics also indicate potential for enhanced skin permeation and retention.

Overall, the nanochitosan-Plai formulation not only retained but potentially enhanced the anti-inflammatory efficacy of the crude extract, making it a promising candidate for future transdermal or topical drug delivery systems. These findings highlight the potential to further develop this formulation into advanced, natural-based therapeutic products such as sprays, patches, or medicated films for localized inflammation management.

## Competing Interests

The authors declare that they have no competing interests.

## Sources of Funding

The authors sincerely acknowledge the financial support provided by Suranaree University of Technology (SUT), Thailand Science Research and Innovation (TSRI), and the National Science, Research, and Innovation Fund (NSRF) (NRIIS number 195617). The authors are also grateful to the Parasitic Diseases Research Center (PDRC) for providing the essential laboratory facilities that were crucial for the successful execution of this study.

## References

1. Koontongkaew S, Poachanukoon O, Sireeratawong S, Dechatiwongse Na Ayudhya T, Khonsung P, Jaijoy K, Soawakontha R, Chanchai M. Safety Evaluation of *Zingiber cassumunar* Roxb. Rhizome Extract: Acute and Chronic Toxicity Studies in Rats. *Int Sch Res Notices*. 2014 Nov 16;2014:632608. doi: 10.1155/2014/632608. PMID: 27379341; PMCID: PMC4897215.
2. Chongmelaxme B, Sruamsiri R, Dilokthornsakul P, Dhippayom T, Kongkaew C, Saokaew S, Chuthaputti A, Chaiyakunapruk N. Clinical effects of *Zingiber cassumunar* (Plai): A systematic review. *Complement Ther Med*. 2017 Dec;35:70-77. doi: 10.1016/j.ctim.2017.09.009. Epub 2017 Oct 7. PMID: 29154071.
3. Jeenapongsa R, Yoovathaworn K, Sriwatanakul KM, Pongprayoon U, Sriwatanakul K. Anti-inflammatory activity of (E)-1-(3,4-dimethoxyphenyl) butadiene from *Zingiber cassumunar* Roxb. *J Ethnopharmacol*. 2003 Aug;87(2-3):143-8. doi: 10.1016/s0378-8741(03)00098-9. PMID: 12860299.
4. Kato E, Kubo M, Okamoto Y, Matsunaga Y, Kyo H, Suzuki N, Uebaba K, Fukuyama Y. Safety Assessment of Bangle (*Zingiber purpureum* Rosc.) Rhizome Extract: Acute and Chronic Studies in Rats and Clinical Studies in Human. *ACS Omega*. 2018 Nov 30;3(11):15879-15889. doi: 10.1021/acsomega.8b02485. Epub 2018 Nov 21. PMID: 30556016; PMCID: PMC6288899.
5. Sinsup P, Teeranachaideekul V, Makarasen A, Chuenchom L, Prajongtat P, Techasakul S, Yingyuad P, Dechtrirat D. *Zingiber cassumunar* Roxb. Essential Oil-Loaded Electrospun Poly(lactic acid)/Poly(ethylene oxide) Fiber Blend Membrane for Antibacterial Wound Dressing Application. *Membranes (Basel)*. 2021 Aug 24;11(9):648. doi: 10.3390/membranes11090648. PMID: 34564465; PMCID: PMC8470900.
6. Ozaki Y, Kawahara N, Harada M. Anti-inflammatory effect of *Zingiber cassumunar* Roxb. and its active principles. *Chem Pharm Bull (Tokyo)*. 1991 Sep;39(9):2353-6. doi: 10.1248/cpb.39.2353. PMID: 1804548.
7. Anasamy T, Abdul AB, Sukari MA, Abdelwahab SI, Mohan S, Kamalidehghan B, et al. A phenylbutenoid dimer, cis-3-(3', 4'-Dimethoxyphenyl)-4-[(E)-3'', 4''-dimethoxystyryl] cyclohex-1-ene, exhibits apoptogenic properties in T-acute lymphoblastic leukemia cells via induction of p53-independent mitochondrial signalling pathway. *Evidence-Based Complementary and Alternative Medicine*. 2013;2013(1):939810.
8. Tanticharoenwivat P, Kulalert P, Dechatiwongse Na Ayudhya T, Koontongkaew S, Jiratchariyakul W, Soawakontha R, Booncong P, Poachanukoon O. Inhibitory effect of Phlai capsules on skin test responses among allergic rhinitis patients: a randomized, three-way crossover study. *J Integr Med*. 2017 Nov;15(6):462-468. doi: 10.1016/S2095-4964(17)60353-4. PMID: 29103416.
9. Chongmelaxme B, Sruamsiri R, Dilokthornsakul P, Dhippayom T, Kongkaew C, Saokaew S, Chuthaputti A, Chaiyakunapruk N. Clinical effects of *Zingiber cassumunar* (Plai): A systematic review. *Complement Ther Med*. 2017 Dec;35:70-77. doi: 10.1016/j.ctim.2017.09.009. Epub 2017 Oct 7. PMID: 29154071.



10. Ozaki Y, Kawahara N, Harada M. Anti-inflammatory effect of *Zingiber cassumunar* Roxb. and its active principles. *Chem Pharm Bull (Tokyo)*. 1991 Sep;39(9):2353-6. doi: 10.1248/cpb.39.2353. PMID: 1804548.
11. Gundom T, Sukketsiri W, Panichayupakaranant P. Phytochemical analysis and biological effects of *Zingiber cassumunar* extract and three phenylbutenoids: targeting NF- $\kappa$ B, Akt/MAPK, and caspase-3 pathways. *BMC Complement Med Ther*. 2025 May 16;25(1):180. doi: 10.1186/s12906-025-04907-w. PMID: 40380132; PMCID: PMC12083117.
12. Luesakul U, Puthong S, Sansanaphongpricha K, Muangsin N. Quaternized chitosan-coated nanoemulsions: A novel platform for improving the stability, anti-inflammatory, anti-cancer and transdermal properties of Plai extract. *Carbohydr Polym*. 2020 Feb 15;230:115625. doi: 10.1016/j.carbp.2019.115625. Epub 2019 Nov 15. PMID: 31887856.
13. Devkota HP, Paudel KR, Hassan MM, Dirar AI, Das N, Adhikari-Devkota A, et al. Bioactive compounds from *Zingiber montanum* and their pharmacological activities with focus on zerumbone. *Applied Sciences*. 2021;11(21):10205.
14. Jiménez-Gómez CP, Cecilia JA. Chitosan: A Natural Biopolymer with a Wide and Varied Range of Applications. *Molecules*. 2020 Sep 1;25(17):3981. doi: 10.3390/molecules25173981. PMID: 32882899; PMCID: PMC7504732.
15. Jiménez-Gómez CP, Cecilia JA. Chitosan: A Natural Biopolymer with a Wide and Varied Range of Applications. *Molecules*. 2020 Sep 1;25(17):3981. doi: 10.3390/molecules25173981. PMID: 32882899; PMCID: PMC7504732.
16. Naveedunissa S, Meenalotchani R, Manisha M, Ankul Singh S, Nirenjen S, Anitha K, et al. Advances in chitosan-based nanocarriers for targeted wound healing therapies: a review. *Carbohydrate Polymer Technologies and Applications*. 2025;11:100891.
17. Gonciarz W, Balcerczak E, Brzeziński M, Jeleń A, Pietrzyk-Brzezińska AJ, Narayanan VHB, Chmiela M. Chitosan-based formulations for therapeutic applications. A recent overview. *J Biomed Sci*. 2025 Jul 8;32(1):62. doi: 10.1186/s12929-025-01161-7. PMID: 40629425; PMCID: PMC12239286.
18. Negi A, Kesari KK. Chitosan Nanoparticle Encapsulation of Antibacterial Essential Oils. *Micromachines (Basel)*. 2022 Aug 6;13(8):1265. doi: 10.3390/mi13081265. PMID: 36014186; PMCID: PMC9415589.
19. Chaowalit Monton JS, Natawat Chankana, Apirak Sakunpak. Applications of Chitosan Nanoparticles and Microparticles for Herbal Medicinal Drug Delivery Systems. *Thai Science and Technology Journal*. 2014:571-81.
20. Hoang NH, Le Thanh T, Sangpueak R, Treekoon J, Saengchan C, Thepbandit W, Papathoti NK, Kamkaew A, Buensanteai N. Chitosan Nanoparticles-Based Ionic Gelation Method: A Promising Candidate for Plant Disease Management. *Polymers (Basel)*. 2022 Feb 9;14(4):662. doi: 10.3390/polym14040662. PMID: 35215574; PMCID: PMC8876194.
21. Sottiwilaiphong JAD. Nano-biopesticide development of betel extract-nano chitosan encapsulated for soft rot control of Chinese cabbage. *Thai Journal of Science and Technology*. 2018;7(5):516-33.
22. Jaiboonma A, Kaokaen P, Chaicharoenaudomrung N, Kunhorm P, Janebodin K, Noisa P, Jitprasertwong P. Cordycepin attenuates Salivary Hypofunction through the Prevention of Oxidative Stress in Human Submandibular Gland Cells. *Int J Med Sci*. 2020 Jul 6;17(12):1733-1743. doi: 10.7150/ijms.46707. PMID: 32714076; PMCID: PMC7378660.
23. Padmanabhan P, Jangle S. Evaluation of in-vitro anti-inflammatory activity of herbal preparation, a combination of four medicinal plants. *International Journal of Basic and Applied Medical Sciences*. 2012;2(1):109-16.
24. Pithayanukul P, Tubprasert J, Wuthi-Udomlert M. In vitro antimicrobial activity of *Zingiber cassumunar* (Plai) oil and a 5% Plai oil gel. *Phytother Res*. 2007 Feb;21(2):164-9. doi: 10.1002/ptr.2048. PMID: 17128430.
25. Suksaeree J, Charoenchai L, Madaka F, Monton C, Sakunpak A, Charoonratana T, et al. *Zingiber cassumunar* blended patches for skin application: Formulation, physiochemical properties, and *in vitro* studies. *Asian Journal of Pharmaceutical Sciences*. 2015;10.
26. Singsai K, Charoongchit P, Utsintong M. The comparison of the oil types in Plai (*Zingiber cassumunar*) oil extraction and analysis of the chemical constituents in Plai oil by gas chromatography-mass spectrometry technique. *Naresaun Phayao J*. 2022;15(3):18-2.
27. Kurita K. Chemistry and application of chitin and chitosan. *Polymer Degradation and Stability*. 1998;59(1-3):117-20.
28. Panthong A, Kanjanapothi D, Niwatananun V, Tuntiwachwuttikul P, Reutrakul V. Anti-inflammatory activity of compounds isolated from *Zingiber cassumunar*. *Planta Medica*. 1990;56(06):655-.
29. Owczarek M, Herczyńska L, Sitarek P, Kowalczyk T, Synowiec E, Śliwiński T, Krucińska I. Chitosan Nanoparticles-Preparation, Characterization and Their Combination with Ginkgo biloba Extract in Preliminary *In Vitro* Studies. *Molecules*. 2023 Jun 23;28(13):4950. doi: 10.3390/molecules28134950. PMID: 37446611; PMCID: PMC10343372.